Electronic Supplementary Information
Wetting and cavitation pathways on
nanodecorated surfaces

Matteo Amabili[1], Emanuele Lisi[1], Alberto Giacomello[1], & Carlo M. Casciola[1]

1. Dipartimento di Ingegneria Meccanica e Aerospaziale, Università di Roma
   "La Sapienza", Rome, Italy

1 Molecular Dynamics
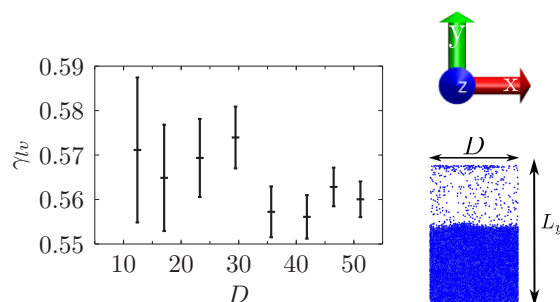
1.1 Liquid-vapor surface tension

Figure S1: Surface tension γ_{lv} of the liquid-vapor interface as a function of the width D of the simulation box. The simulations are for a Lennard-Jones fluid at $T = 0.8 \, \varepsilon/k_B$.

The liquid-vapor surface tension γ_{lv} is estimated via equilibrium molecular dynamics (MD) simulations of liquid-vapor slabs (see the right panel of Fig. S1). Fluid particles interact via the Lennard-Jones potential defined in the main text. The system is kept at constant temperature $T = 0.8 \, \varepsilon/k_B$ using a Nosé-Hoover chain thermostat. Periodic boundary conditions are applied in the three directions.

The surface tension γ_{lv} is estimated following Kirkwood and Buff[1]:

$$\gamma_{lv} = \frac{1}{2} L_y (P_N - P_T) \, , \tag{1}$$

where L_y is the dimension of the simulation box in y direction (Fig. S1) and P_N (P_T) is the component of the pressure tensor $P_{\alpha\beta}$ normal (tangential) to the interface. The factor 1/2 in eqn (1) follows from the presence of two liquid-vapor

interfaces due to the periodic boundary conditions. In our simulations P_N and P_T read as follow:

$$P_N = P_{yy} \tag{2a}$$

$$P_Y = \frac{1}{2}(P_{xx} + P_{zz}) \ . \tag{2b}$$

The components P_{xx}, P_{yy}, and P_{zz} of the pressure tensor can be evaluated in MD simulations using the virial expression[2]:

$$P_{\alpha\beta} = \frac{1}{V} \left\langle \sum_{i=1}^{N} m v_\alpha^i v_\beta^i + r_\alpha^i f_\beta^i \right\rangle \ , \tag{3}$$

where $V = D^2 L_y$ is the total volume of the simulation box with $L_x = L_z \equiv D$. The sum in eqn (3) extends over the total number of particles, N, while r_α^i, v_α^i, f_α^i are the α-components of the position, velocity, and force of the i-th particle, respectively.

The values of γ_{lv} as a function of the width D of the simulation box are shown in Fig. S1 and are found to be practically independent of the size of the liquid-vapor interface up to the investigated scale. The estimated value of the liquid-vapor surface tension is $\gamma_{lv} = 0.57 \pm 0.02 \ \varepsilon/\sigma^2$.

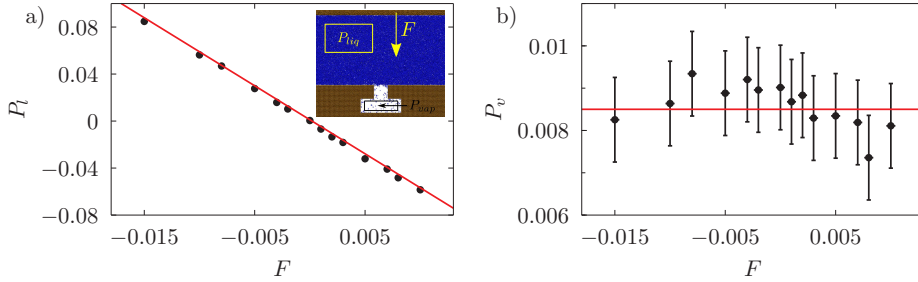## 1.2 Computation of the pressure

Figure S2: a) Liquid pressure P_l as a function of the force F acting on the atoms of the upper wall (black symbols); the error bars are smaller than the symbol size. The red line is eqn (4). The inset shows a snapshot of the atomistic system, with the yellow (black) box indicating the region in which P_l (P_v) is computed from eqn (3) and eqn (5). b) Vapor pressure P_v as a function of the force F; the red line represents the average value.

In this subsection we describe the procedure used in MD to estimate the liquid and vapor pressures P_l and P_v, respectively. These are needed in order to compare atomistic and macroscopic results at the same thermodynamic conditions. As already mentioned in the main text, the upper solid wall of the system is used as a piston in order to control the liquid pressure (see Fig. S2a). This is obtained by applying a constant force F in the y direction to each particle in the wall. At equilibrium, the total force on the upper wall is balanced by the liquid pressure:

$$F N_p = P_l A \ , \tag{4}$$

where N_p is the number of particles in the upper wall and $A = L_x L_z$ is its surface area. In the simulations P_l is also estimated independently by computing the pressure tensor $P_{\alpha\beta}$, defined in eqn. (3), in a suitable control region (the yellow box in the inset of Fig. S2) and defining

$$P_l = (P_{xx} + P_{yy} + P_{zz})/3 \ . \tag{5}$$

In Fig. S2a, P_l is reported as a function of the applied force F. As expected from eqn (4) a linear relation holds. The negative sign of the angular coefficient is due to the y-axis which is oriented in the opposite direction of F. Thus a positive force F corresponds to a negative pressure (tensile state).

A similar procedure can be applied to compute the vapor pressure P_v. In this case the control region for the computation of the pressure tensor is the black box in the inset of Fig. S2a. P_v is always computed in the Cassie state to ensure that the liquid-vapor interface is far from the control region. Figure S2b reports P_v as a function of the force F. This result shows that the vapor pressure does not depend on F (hence on P_l) and can be safely considered constant (for the chosen temperature $T = 0.8 \ \varepsilon/k_B$). The average value of the vapor pressure is $P_v = 0.0084 \ \varepsilon/\sigma^3$.

Given $P_l(F)$ and P_v it is straightforward to compute $\Delta P(F) = P_l(F) - P_v$ which is needed as an input for the macroscopic model.

2 Surface Evolver calculations

In the present section some technical details are reported in order to clarify the use of Surface Evolver[3] in solving the CREaM equations. The *"Surface Evolver"* (SE in the following) is a computational tool which allows one to find minimal surfaces, that is, surfaces that minimize their surface energy subject to imposed constraints. The surfaces can be subjected to various kinds of constraints: the geometrical ones which act on the position of vertices, edges, and facets, i.e., boundary constraints and boundary contact angle; and the "integrated quantity" ones which act on quantities such as the body volume. The final equilibrium shape of the liquid-vapor interfaces and the related surface energy come out from a combination of these factors.

The SE uses a *finite-elements method*, which means that the "surface" under investigation is discretized in a mesh made of simple elements. The initial configuration of the system is manually implemented by the user which defines in a datafile the surfaces and bodies, the boundary and volume constraints and the various energies acting on the system itself.

Since the geometries considered in MD are effectively two-dimensional, given the periodic boundary conditions in the z direction, we use the SE with one-dimensional "surfaces" in two-dimensional space which is implemented in the so-called *string model*[3]. The basic element of this model is a segment and the surface tension resides in these one-dimensional elements.

The SE evolves the surface towards minimal energy following a *gradient descent method*. At every iteration step the algorithm reduces energy while obeying the imposed constraints. The algorithm calculates the force acting on each vertex as the negative gradient of the total energy. Subsequently the surface is changed moving the free vertices in the direction of the force.

In the case under investigation SE allows one to study the possible shapes that a cavitation bubble assumes in different stages of growth. The SE is very useful because the possible shapes of the vapor domains become complex given the re-entrant geometry of the cavity and its heterogeneous chemistry.
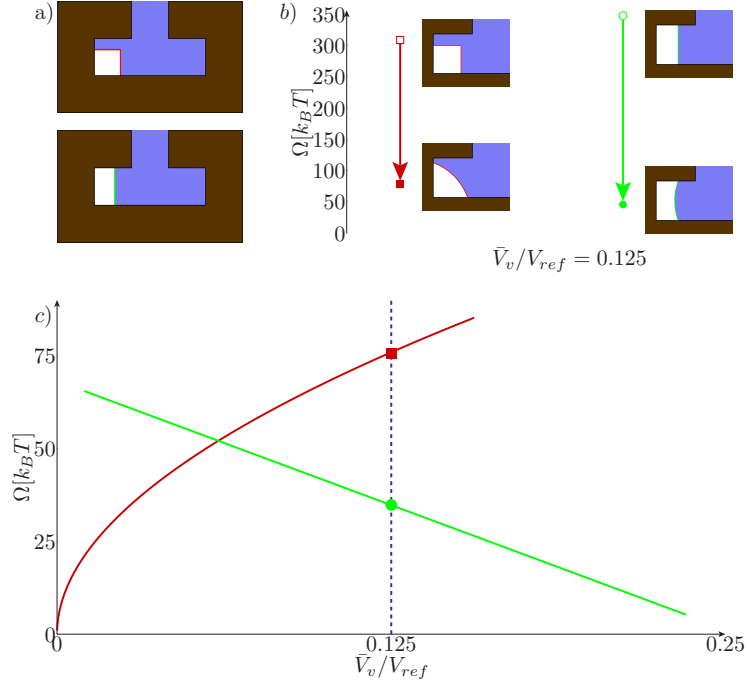
2.1 Free-energy calculations

Figure S3: Illustration of the procedure followed to obtain the free-energy profiles via CREaM. a) two different topologies, vapor bubble in a corner and a symmetric meniscus inside a branch of the T-shaped defect, are selected. b) minimization via SE for a fixed value of the vapor volume: the shape of the liquid-vapor interface evolves in order to reach the constrained free-energy minimum. c) free-energy profiles as a function of $\bar{V}_v$ for the two selected topologies; the points correspond to the free-energies computed in panel b).

In CREaM calculations the liquid-vapor surface tension is set equal to that computed in MD simulations and the relation between solid-liquid, solid-vapor, and liquid-vapor surface tensions is imposed via the Young's equation. For the hydrophobic (hydrophilic) chemistry the contact angle of the liquid-vapor interface is $\theta_Y = 110°$ ($\theta_Y = 55°$).

The SE is used in order to find the configuration corresponding to free-energy minima which enclose a given volume of vapor $\bar{V}_v$. These configurations coincide with the solutions of eqn (5) of the main text (CREaM); this procedure, however, yields only the constrained minima. The free-energy profile is then obtained by evaluating the surface contribution $\Omega^{(s)} = \gamma_{lv}(A_{lv} + \cos\theta_Y A_{sv})$ in eqn (3) of the main text for the minimal surfaces enclosing $\bar{V}_v$ computed by SE; this procedure is repeated for all $\bar{V}_v$ ranging from the pure liquid to the pure
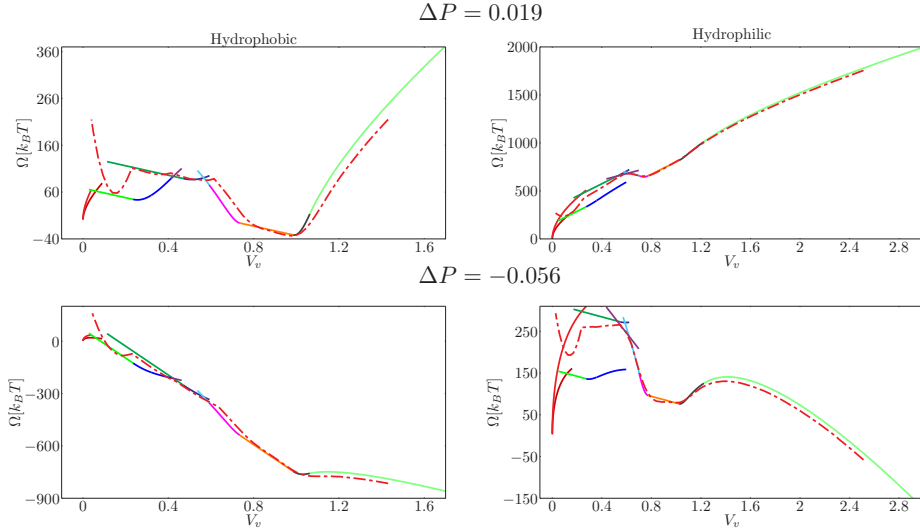
Figure S4: Free-energy profiles computed via SE at different pressures (solid lines). Two chemistries, hydrophobic and hydrophilic, are reported in the left and right panels, respectively. Figures on the top panels refer to $\Delta P = 0.19$, those on the bottom to $\Delta P = -0.056$. The corresponding atomistic free-energy profiles are reported for comparison (dash-dotted lines).

vapor states. The only delicate point is that for a given $\bar{V}_v$ there are several different bubble shapes that satisfy CREaM conditions; we try to compute all of them in order to be able to compare the free energies connected to each of these "valleys" of the free-energy landscape. From an operational point of view the procedure, illustrated in Fig. S3, consists of the following steps:

a) identify the possible topologies that a vapor domain can assume (see Fig. S3a);

b) find via SE the minimal solution corresponding to the chosen bubble topology at fixed $\bar{V}_v$ (see Fig. S3b);

c) evaluate the surface free-energy profile $\Omega^{(s)}(V, T; \bar{V}_v)$ as function of the volume of vapor ranging from $\bar{V}_v = 0$ to $\bar{V}_v \gg V_{ref}$ (see Fig. S3c);

d) repeat the last two steps for every bubble topology.

It is important to remark that the minimization procedure implied in CREaM and implemented in the SE calculations involves *only* the surface terms[4]. As already clear from eqn (3) of the main text, the pressure term is simply a linear term in $\bar{V}_v$ which is added to the surface free-energy profile:

$$\Omega(\mu, V, T; \bar{V}_v) = \Omega^{(s)}(V, T; \bar{V}_v) - \Delta P(\mu) \, \bar{V}_v \ . \qquad (6)$$

In the main text profiles at $\Delta P = 0$ are reported. In Fig. S4 representative profiles at positive and negative ΔP are shown.

References

[1] J. G. Kirkwood and F. P. Buff, *The Journal of Chemical Physics*, 1949, **17**, 338–343.

[2] S. Nosé and M. Klein, *Molecular Physics*, 1983, **50**, 1055–1076.

[3] K. A. Brakke, *Experim. Math.*, 1992, **1**, 141–165.

[4] A. Giacomello, M. Chinappi, S. Meloni and C. M. Casciola, *Phys. Rev. Lett.*, 2012, **109**, 226102.